Photoluminescence and Förster resonance energy transfer in elemental bundles of single-walled carbon nanotubes

Lefebvre, Jacques; Finnie, Paul

Publisher's version / Version de l'éditeur:
https://doi.org/10.1021/jp810892z
The Journal of Physical Chemistry C, 113, 18, p. 7536–7540, 2009-04-09

Photoluminescence and Förster Resonance Energy Transfer in Elemental Bundles of Single-Walled Carbon Nanotubes

Jacques Lefebvre* and Paul Finnie

Institute for Microstructural Sciences, National Research Council, Ottawa, ON, Canada, K1A 0R6

Received: December 10, 2008; Revised Manuscript Received: February 24, 2009

Single-walled carbon nanotubes (SWNTs) are commonly synthesized in bundles for which the luminescence is often quenched altogether. Here, we report on the simplest case of nanotube bundles: a single pair of individual air-suspended SWNTs. Using luminescence imaging spectroscopy, we find that emission and excitation spectra can be described within an energy transfer picture, with donor to acceptor transfer of excitation. The multiplicity of emission peaks in small bundles indicates that the transfer of luminescence is only partial at room temperature, with thermal occupation of the donor being significant. We attribute this signature to the unique band structure of SWNTs, with diameter and chirality dependent energy, recombination rate, and density of states.

Introduction

Single-walled carbon nanotubes (SWNTs) are luminescent when properly isolated from other nanotubes and surfaces.[1,2] However, SWNTs are commonly synthesized in bundles, for which there is a common misconception that luminescence is quenched altogether. Recently, a few studies have addressed the luminescence from SWNT bundles and revealed a signature of energy transfer to SWNTs with the lowest energy.[3−6]

Förster resonance energy transfer (FRET) is an important research topic with direct applicability to biological systems[7] and potential impact for the design of light emitting or harvesting devices.[8] In FRET,[9] electronic excitations in a fluorescent donor (D) molecule transfer to an acceptor (A) molecule, which shows fluorescence at lower energy (see ref 10 for a general review). The efficiency of the FRET process depends on the spectral overlap between donor and acceptor molecules. This transfer is understood to occur without exchange of photons, being instead the result of dipole−dipole coupling. The extent of the transfer is long ranged and falls off as the sixth power of D−A separation for point dipoles, with a characteristic Förster distance of a few nanometers.

In several ways, SWNTs possess the attributes of a FRET system. For one, individually isolated semiconducting SWNTs are excellent fluorophores, meaning that when photoexcited they emit photoluminescence (PL), more precisely termed fluorescence. For a general overview of SWNT PL, see ref 11. Properly prepared, SWNTs have excellent photostability and relatively high quantum yield (∼10%). In addition, the sharp infrared PL emission peak (∼10 nm FWHM at ∼1 μm) is broadly tunable (0.8 μm to wavelengths longer than 2.2 μm), together with a continuous absorption spectrum above the PL peak, with sharp absorption peaks in the near-infrared, visible, and ultraviolet range (∼30 nm FWHM at ∼600 nm). The emission and absorption spectra are determined mainly by the SWNT species, each with a discrete, well-defined diameter and chirality. Each combination of nanotube species should be viewed as a D−A pair where FRET processes operate. As a one-dimensional material, the SWNT has a continuous density of states above the band gap. Therefore, the spectral overlap required for FRET occurs at all energies above both band gaps for any pair of SWNTs. The intimate contact between individual nanotubes in a bundle (spacings on the order of the stacking of graphite, ∼0.34 nm) leads to the expectation of very high FRET efficiencies (close to unity). This also means that (Dexter) charge transfer might also play some role in parallel with FRET.

Results and Discussion

Contrary to the above expectation, SWNTs synthesized in bundles generally show only very weak and nearly featureless light emission. This degradation in spectral properties has correctly been attributed to nonradiative recombination in metallic SWNT constituents of bundles.[1] Bundles comprising only semiconducting SWNTs have always been expected to emit structured PL. However, all-semiconducting bundles become quite rare as the bundle size increases. This is because, for a broad and random (n,m) distribution, 1/3 of the possible species are metallic and so the probability of having an all-semiconductor bundle is $2/3^N$, where N is the number of nanotubes in a bundle.

Recently, there have been reports investigating the effect of controlled bundling starting from a solution of isolated SWNTs with bright PL.[3,4] The changes noted in photoluminescence excitation (PLE) maps upon bundling was attributed to exciton transfer between species. An important limitation in those studies is the ambiguity inherent to ensemble measurements, where interpretation can be complicated by overlapping contributions from several SWNT species. Furthermore, the degree of bundling in such samples is typically not well-characterized. At the individual nanotube level, near-field imaging studies show clear evidence of exciton transfer between two adjacent SWNTs.[5] In all of these studies, the PL intensity of the higher band gap SWNT was reportedly transferred to the lower band gap SWNT, giving rise to an extra feature in the PLE map.

In this work, we use long (> 10 μm) near-ideal air-suspended SWNTs and combine PL imaging and PLE mapping techniques to show systematically how bundling affects the optical spectra. The measurements are performed on single elemental bundles with minimum ambiguity in spectral assignment. We compare

* To whom correspondence should be addressed. E-mail: jacques.lefebvre@nrc.ca.

10.1021/jp810892z CCC: $40.75 Published 2009 by the American Chemical Society
Published on Web 04/09/2009

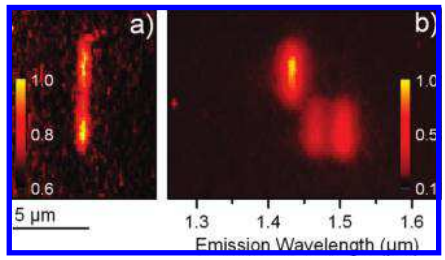

Figure 1. Photoluminescence (PL) imaging spectroscopy of an elemental SWNT bundle. (a) PL image from a ~10 μm long segment. (b) The same image spectrally dispersed, showing a single PL peak for the upper segment (1.43 μm), and twin emission peaks for the lower segment (1.46 and 1.51 μm).

the PLE map of bundled and unbundled segments of the same SWNT to directly reveal extra PL features arising from FRET processes. We show the structure dependence of these features and show systematically how these vary from single SWNTs to pairs, triplets, and up to quadruplet (i.e., bundles of 2, 3, and 4 SWNTs).

For this study, long nanotubes (≫10 μm) were grown by chemical vapor deposition directly on a lithographically fabricated grating pattern in thermal oxide on silicon substrates. Nanotube yield, a function of catalyst loading and growth conditions, was low enough that many individual SWNTs were formed but high enough that many formed bundles. Nanotubes grew from the top of the mesas, and many bridged the trenches, which were ~10 μm in length. The trenches provide a region over which the nanotube is suspended, free from the quenching effect of direct contact with the substrate.[2,12] In many cases, the same nanotube bridged multiple trenches. The PL was imaged with a home-built near-infrared microscope, using a defocused tunable cw Ti:sapphire laser for illumination and a grating to obtain a spatially resolved PL spectrum.[14] PL imaging spectroscopy in the far field is a proven, powerful tool for the study of individual SWNTs.[13−17]

Experimental details have been described in previous reports.[15,16] The fluorescence, excited with a tunable Ti:sapphire laser (polarized parallel to nanotube), was dispersed on a 100 lines/mm grating and focused (20 cm focal length) on a 256 × 1024 InGaAs camera. The low wavelength dispersion achieved with this system (2.7 nm/pixel) allows for simultaneous nondispersive imaging at zeroth order and imaging spectroscopy at first order. The sample was rotated to ensure that the straight nanotube segments were always parallel to the grating grooves and vertical on the camera.

An image of a single structure suspended in two segments is shown in Figure 1a. When spectrally resolved, the large majority (>90%) of such isolated segments showed a single PL peak (E_{11}). This is indeed the case for the upper segment of Figure 1a. Its spectrally resolved image in Figure 1b shows a single emission peak at 1.43 μm. On the other hand, the bottom segment in Figure 1a has two emission peaks (1.46 and 1.51 μm in Figure 1b). We attribute this spectral signature to an isolated SWNT (upper segment) contacting another SWNT to form a two nanotube bundle (bottom segment).

This is supported by PLE maps obtained from each segment. As shown in Figure 2a, the single nanotube segment is dominated by a single spot, the result of resonant excitation at E_{22} and emission at E_{11}.[18] From the peak position, the upper segment is assigned to an individual (10,8) SWNT.

The lower segment (Figure 2b) shows four peaks in the PLE map, in a characteristic rectangular pattern of two E_{11} and two E_{22} values. We will show that this is the PLE signature of

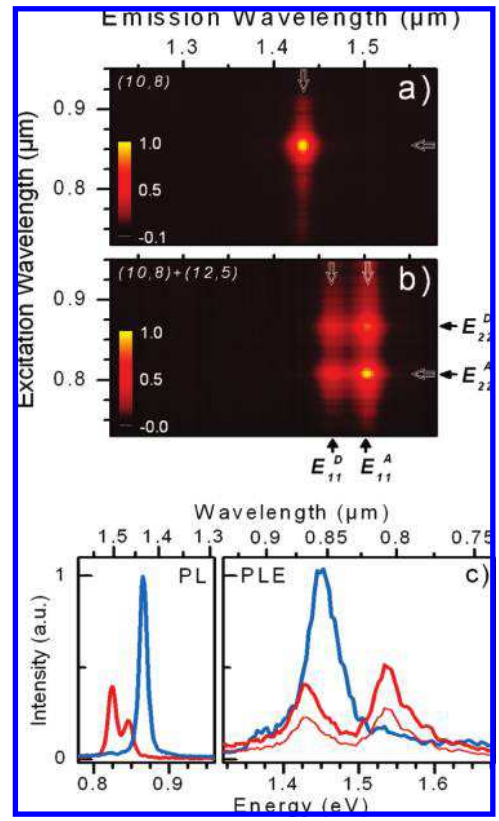

Figure 2. Spectral signature of a two nanotube bundle. (a) The photoluminescence excitation (PLE) map taken from the upper segment in Figure 1 showing the spectral signature of a single (10,8) SWNT. (b) The PLE map taken from the lower segment in Figure 1 showing the spectral signature of a two nanotube bundle, a (10,8) with a (12,5) SWNT. The labels E_{11}^D, E_{11}^A, E_{22}^D, and E_{22}^A indicate the origin of each spectral feature. The (10,8) nanotube is of donor type in the bundle. (c) Slices taken from (a) and (b) [open arrows, with horizontal slices for PL (left panel) and vertical slices for PLE (right panel)] provide a direct comparison between a single nanotube (blue) and a two nanotube bundle (red). A 19 meV red shift of E_{11} occurs upon bundling. Relative intensities have not been normalized and are representative of the efficiency of the transfer process.

bundling between two SWNTs. For two unbundled nanotubes of different species, we can expect two independent (E_{11}, E_{22}) pairs. Both spots should persist within a bundle unless the spectral weight of the donor is 100% transferred to the acceptor. These states are labeled (E_{11}^D, E_{22}^D) and (E_{11}^A, E_{22}^A), with the superscript D and A for donor and acceptor, respectively. The donor is the nanotube with the larger E_{11}, the acceptor is the one with the smaller E_{11}. The brightest spot in the PLE map is assigned to (E_{11}^A, E_{22}^A), while the spot diagonal to it is (E_{11}^D, E_{22}^D). The energy transfer process between nanotubes within a bundle also gives rise to two additional resonances, (E_{11}^A, E_{22}^D) and (E_{11}^D, E_{22}^A), where emission in one nanotube follows from excitation in the other. These peaks are a unique signature of SWNT bundles.

Specific assignment for Figure 2b goes as follows. The weak top left peak (1.46 μm, 865 nm) in the bundle PLE is the same peak as the isolated SWNT. This corresponds to (E_{11}^D, E_{22}^D) excitation and emission from a (10,8) nanotube which acts as a donor of excitons to the other member of the bundle. Upon bundling, the E_{11} and E_{22} energies of the (10,8) nanotube are red-shifted by approximately 20 meV, as seen in Figure 1c. This red shift can be attributed to a change in dielectric environment produced by the neighboring nanotube.[16,19] Upon bundling, similar red shifts have also been observed by Rayleigh scattering

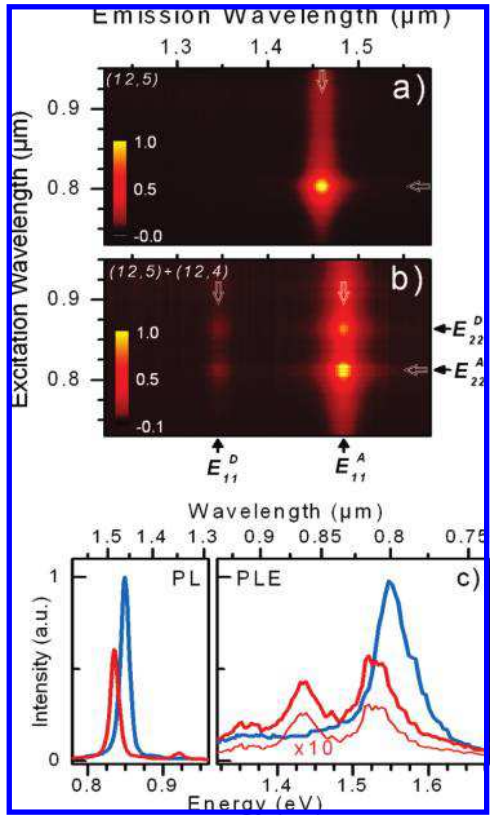

Figure 3. A second example of a two nanotube bundle, with the isolated nanotube being of acceptor type in the bundle. PLE maps from the isolated and bundled nanotube segment are shown in (a) and (b), respectively. The labels E_{11}^{D}, E_{11}^{A}, E_{22}^{D} and E_{22}^{A} indicate the origin of each spectral feature. (c) Slices taken from (a) and (b) [open arrows, with horizontal slices for PL (left panel) and vertical slices for PLE (right panel)] provide a direct comparison between a single nanotube (blue) and a two nanotube bundle (red). A 21 meV red shift of E_{11} is seen upon bundling. Relative intensities have not been normalized and are representative of the efficiency of the transfer process.

(E_{33} and E_{44} transitions)[20] and by near-field spectroscopy.[5] Although the magnitude of the shifts is comparable, the different experimental conditions (e.g., smaller or larger nanotube diameter, and differing dielectric environments) make direct comparisons difficult.

In the rectangular pattern of Figure 2b, the PLE peak diagonal to (E_{11}^{D}, E_{22}^{D}) is (E_{11}^{A}, E_{22}^{A}) with emission at 1.51 μm and maximum excitation at 800 nm (at $E_{11} = 0.82$ eV and $E_{22} = 1.54$ eV). As the acceptor molecule, this is the dominant peak in the PLE map. It can be assigned to a (12,5) nanotube once a 20−30 meV red shift is accounted for (from our previous work, the (12,5) is expected at $E_{11} = 0.857$ eV and $E_{22} = 1.567$ eV). The off-diagonal peaks in Figure 2b correspond to (E_{11}^{A}, E_{22}^{D}) and (E_{11}^{D}, E_{22}^{A}) where absorption from either nanotube in the bundle leads to emission in the other nanotube.

Figure 3 presents a second example, but where the isolated nanotube is of acceptor type. The PLE map of the isolated SWNT (Figure 3a) is assigned to the (12,5) species (PL at 1.46 μm). In Figure 3b, the PLE map from the same SWNT in a bundle is red-shifted due to dielectric screening. Here, it pairs with a (12,4) SWNT (PL at 1.34 μm in Figure 3a), with a larger band gap. The rectangular pattern is also visible with (E_{11}^{A}, E_{22}^{A}) being the dominant peak, similar to Figure 2b. The emission from the donor (12,4) SWNT is much weaker compared to the case of Figure 1b. We attribute this difference to the larger energy splitting between E_{11}^{D} and E_{11}^{A} compared to the first example, 76 versus 28 meV. This point will be discussed in detail later.

Of importance to FRET is whether the luminescence is enhanced in the process. We shall see that it leads to a relative enhancement of luminescence for excitation at certain specific energies, but to an absolute loss in luminescence intensity. The PLE maps in Figures 2 and 3 have been normalized separately to their maximum intensities, and so comparing the maps does not properly represent any enhancement effects. To do so, the relative intensities are plotted in Figures 2c and 3c with PLE slices taken at the E_{11} energies (vertical arrows in Figures 2a,b and 3a,b). Within a multiplication factor, PLE slices taken at E_{11}^{D} and E_{11}^{A} appear identical. This implies that the rate of D−A and A−D exciton transfer is much faster than the rate of exciton recombination. The system effectively loses the memory of whether it was excited into donor or acceptor states.

In both Figures 2c and 3c, the isolated nanotube is significantly brighter than the bundle, with about twice the intensity of the bundle. This indicates that, upon bundling, a small fraction of excitons are lost nonradiatively. Exciton transfer leads to an absolute loss in luminescence efficiency. The precise origin of nonradiative decay in SWNTs remains an open question; however, an explanation based on defect-mediated exciton recombination is consistent with the present result. If the rate of nonradiative decay scales with the number of defects per unit length, an exciton within a bundled pair of SWNTs effectively interacts with twice as many defects per unit length as it would in a single isolated SWNT (i.e., assuming the defect densities are the same for all nanotubes).

Despite the loss in absolute intensity, it must be recognized that a relative enhancement of PL intensity is still observed, specifically at energies off resonance with respect to E_{22} of the isolated SWNT. Here, this FRET-related PL efficiency enhancement is approximately twofold, as can be seen in Figure 2c, where the luminescence is increased at the donor resonance (around 1.53 eV) as compared to the isolated single (acceptor derived) nanotube. The (12,4) donor SWNT acts as an effective absorption channel at an energy where the (12,5) acceptor SWNT absorbs poorly. This new excitation channel widens the window over which the (12,5) SWNT can be efficiently excited. Such enhancement, coupled with the transfer efficiency dependence on D−A spatial separation, is what makes common FRET fluorophores useful as "spectroscopic rulers". Therefore, in principle, SWNTs could be used in this same way as common FRET fluorophores. In these samples, while this excitation wavelength specific enhancement did occur, at the same time, upon bundling there was a 2-fold reduction in the overall quantum yield. This may not be general. For example, if the loss in quantum yield is defect-mediated, nanotubes with lower defect densities could be less affected upon bundling. However, if bundling is always accompanied by a loss in quantum yield of similar magnitude, bundle engineering would not be a very good strategy to improve light harvesting by donors to increase acceptor PL intensity. Interestingly, here, since the emission intensity is halved, but the absorption doubled, excitation with a broadband (white light) source would produce a similar total PL signal whether the SWNT was isolated or in a (nonmetallic) bundle.

Earlier PLE mapping studies on bundles suggest efficient Förster energy transfer only from the donor to the acceptor nanotube.[3,4] The presence here of two emission peaks appears to conflict with these earlier reports. In Figure 2b, only 50% of the spectral weight is transferred, and this number varies

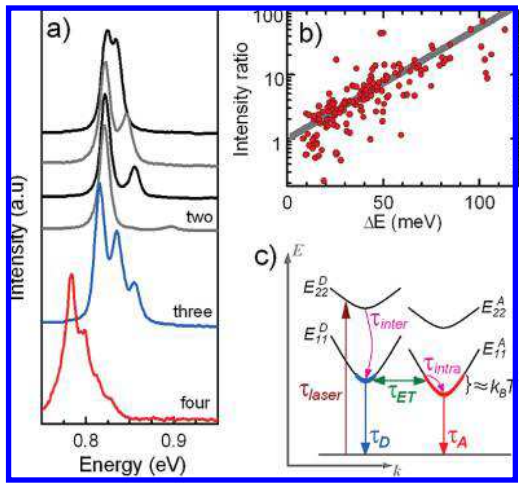

Figure 4. Systematic variation in peak intensities due to the FRET process in bundles. (a) Emission spectra from bundles made of two (black and gray), three (blue), and four (red) nanotubes. The lowest energy peak shows stronger emission intensity, while the intensity of the high energy peak weakens for larger energy separation. (b) Intensity ratio between the low and high energy peak as a function of the energy difference between the peaks, $\Delta E = E_{11}{}^{D} - E_{11}{}^{A}$. The continuous line is a Boltzmann factor $e^{\Delta E/k_BT}$, with $k_BT = 25$ meV. (c) Schematic band structure diagram for the donor and acceptor with the time scales of relevant transitions labeled (see text).

dramatically from bundle to bundle, as Figure 3b shows. Figure 4a shows four examples of emission spectrum from two nanotube bundles. All four bundles have one nanotube with $E_{11}{}^{A} \simeq 0.82$ eV and with the second nanotube having a higher emission energy. We find that the larger the energy difference between the two E_{11}s, the more complete is the transfer of PL intensity. This result is also observed for bundles made of three or four nanotubes, as seen in Figure 4a (blue and red lines).

In ref 5, both PL peaks were observed for bundles, and this was attributed to a fractional efficiency of exciton transfer. Since the distance between SWNTs was varying, that may have been the case, at least for large separations. However, in the present case, the nanotubes in the bundle are in direct contact, and at such short scales, the FRET efficiency is expected to be effectively 100%. Moreover, finite transfer efficiency cannot explain the rectangular pattern of PLE spots.

Figure 4b, summarizing data acquired from over 150 bundles, provides a clue to explain the apparent reduction in transfer efficiency and the origin of "extra" PLE spots. Figure 4b shows a plot of the PL peak intensity ratio $I(E_{11}{}^{A})/I(E_{11}{}^{D})$ as a function of the energy splitting between E_{11}s, $E_{11}{}^{D} - E_{11}{}^{A}$. Albeit with significant scatter, the plot reveals a simple overall scaling with Boltzman factor $e^{\Delta E/k_BT}$, with $k_BT = 25$ meV (that is room temperature). Thus, the finite intensity of the donor PL peak is not attributed to limited efficiency of transfer, but rather to thermal occupation of the donor's emission band. Even with 100% transfer efficiency from donor to acceptor, excitons are transferred back from acceptor to donor if they have sufficient thermal energy. The relative intensity is governed not only by transfer efficiency but also by occupancy.

The effects are summarized in Figure 4c. It shows an energy band diagram with the relevant transitions labeled with their time scales. Resonant excitation is illustrated, whereby the excitation source excites carriers from the ground state to an excited state, here the $E_{22}{}^{D}$ band, with an effective time constant τ_{Laser}. There is a rapid interband relaxation to the donor ground state ($\tau_{Inter} \sim 10-100$ fs) where the exciton can recombine by emission of a photon or hop to the other nanotube. Since the recombination times ($\tau_D, \tau_A \sim 10$ ns) are typically much longer than the exciton transfer time (τ_{ET})[21] and the intraband relaxation time ($\tau_{Intra} \sim 1-10$ fs), excitons are efficiently thermalized before they recombine (a review of exciton dynamics can be found in ref. 22). Thus they are distributed statistically according to the temperature and density of states. The thermal occupation of the E_{11} bands is illustrated schematically in Figure 4c (red and blue segments of the energy dispersions), with the band filled up to $\sim k_BT$ above $E_{11}{}^{A}$.

The significant scatter of data in Figure 4b is beyond experimental uncertainties and may originate in the species dependent variation in density of states and/or recombination time. The density of states is species dependent. Due to trigonal warping, even two SWNTs with similar E_{11} values can have quite different density of states (a (10,8) and a (14,1) for example). Since the PL intensity is proportional to occupation, this alone will cause some scatter. The radiative rate which determines the PL intensity has been shown to be (n,m) dependent,[23−25] and scatter in the ratio is also expected for this reason. The scatter thus provides some information as to the extent that these parameters can vary.

A further consideration is the effect of momentum conservation on the rate of energy transfer, τ_{ET}. For instance, a (9,8) and a (9,7) nanotube have significant momentum mismatch for excitons near E_{11} since their E_{11} energy dispersions are slices originating from opposite sides of the graphene conical dispersion. This should make exciton transfer less effective compared to, for example, a bundle made of a (9,8) and (10,6) nanotube, which are much more closely matched in momentum at E_{11}. Furthermore, some bundles may be well matched by specific phonon distributions, potentially making scattering efficiencies higher for some SWNT pairs. Fully chiral assigned versions of Figure 4c would enable a better understanding of the origin of the scatter in intensity ratio and may provide evidence for momentum matching rules.

Conclusion

The existence of energy transfer and its effects are now clearly established in SWNT bundles. This will be important for a complete understanding of the fundamental optical and electronic properties of SWNTs. Energy transfer should also appear as a new parameter in engineering the optical properties of SWNTs. It must be recognized that while the exciton transfer data here can be understood in terms of the FRET mechanism alone (Dexter) charge transfer likely also occurs in parallel. That said, charge transfer would most likely produce additional spectral features, but here the change to the spectrum is very mild, even preserving line shape and line width. We failed to observe any new spectral features due to bundling, though of course very weak features or features at wavelengths not yet explored cannot be ruled out. A separate line of evidence that the transfer is FRET as opposed to charge transfer comes from electronic theory, which predicts that SWNTs in a bundle do not interact strongly,[26] and so would seem to suggest that FRET should dominate over charge transfer for most SWNT donor−acceptor pairs. Experimentally, the excitation spectrum from a bundle appears to be simply the result of additive contributions from individual SWNT components, and this is significant evidence for FRET over charge transfer.

The SWNT materials system appears to be an ideal model system to explore exciton transfer photophysics with new clarity. For example, since there is an essentially unlimited number of possible (n,m) species, there is a doubly unlimited number of possible donor−acceptor pairs, making SWNTs more versatile

than the majority of FRET fluorophores. As a consequence, and in contrast to most FRET pairs, donor−acceptor pair level splittings can range from zero to over order 1 eV, a range that includes the thermal energy at room temperature (25 meV). SWNTs are compelling fluorophores for FRET also because of their sharply peaked emission and excitation spectra and near-absence of Stokes shift.

The identification of FRET in SWNTs also has great potential for applications. Within the nanotube field, PLE mapping is becoming a routine characterization tool and analysis should be performed with bundling and exciton transfer in mind. Since FRET continues to be a lively research topic with applications in biology, medicine, and optoelectronics more generally, SWNTs have great potential for FRET-related work in these areas.

Acknowledgment. We are grateful to D. G. Austing, P. Chow Chong, K. Kaminska, P. Marshall, and H. Tran for assistance with sample preparation.

References and Notes

(1) O'Connell, M. J.; Bachilo, S. M.; Huffman, C. B.; Moore, V.; Strano, M. S.; Haroz, E.; Rialon, K.; Boul, P. J.; Noon, W. H.; Kittrell, C.; Ma, J.; Hauge, R. H.; Weisman, R. B.; Smalley, R. E. Band Gap Fluorescence from Individual Single-Walled Carbon Nanotubes. *Science* **2002**, *297*, 593–596.

(2) Lefebvre, J.; Homma, Y.; Finnie, P. Bright Band Gap Photoluminescence from Unprocessed Single Walled Carbon Nanotubes. *Phys. Rev. Lett.* **2003**, *90*, 217401.

(3) Torrens, O. N.; Milkie, D. E.; Zheng, M.; Kikkawa, J. M. Photoluminescence from Intertube Carrier Migration in Single-Walled Carbon Nanotube Bundles. *Nano Lett.* **2006**, *12*, 2864–2867.

(4) Tan, P. H.; Rozhin, T. H.; Hu, P.; Scardaci, V.; Milne, W. I.; Ferrari, A. C. Photoluminescence Spectroscopy of Carbon Nanotube Bundles: Evidence for Exciton Energy Transfer. *Phys. Rev. Lett.* **2007**, *99*, 137402.

(5) Qian, H.; Georgi, C.; Anderson, N.; Green, A. A.; Hersam, M. C.; Novotny, L.; Hartschuh, A. Exciton Energy Transfer in Pairs of Single-Walled Carbon Nanotubes. *Nano Lett.* **2008**, *8*, 1363–1367.

(6) Kato, T.; Hatakeyama, R. Exciton Energy Transfer-Assisted Photoluminescence Brightening from Freestanding Single-Walled Carbon Nanotube Bundles. *J. Am. Chem. Soc.* **2008**, *130*, 8101–8107.

(7) Saini, S.; Singh, H.; Bagchi, B. Fluorescence Resonance Energy Transfer (FRET) in Chemistry and Biology: Non-Förster Distance Dependence of the FRET Rate. *J. Chem. Sci.* **2006**, *118*, 23–35.

(8) Moons, E. Conjugated Polymer Blends: Linking Film Morphology to Performance of Light Emitting Diodes and Photodiodes. *J. Phys.: Condens. Matter* **2002**, *14*, 12235–12260.

(9) Förster, Th. 10th SPIERS Memorial Lecture: Transfer Mechanisms of Electronic Excitation. *Discuss. Faraday Soc.* **1959**, *27*, 7–17.

(10) Lakowicz, J. R. *Principles of Fluorescence Spectroscopy*; Springer: New York, 2006; 954 pp.

(11) Jorio, A., Dresselhaus, G., Dresselhaus, M. S., Eds. *Carbon Nanotubes: Advances Topics in the Synthesis, Structure, Properties and Applications, Topics in Applied Physics*; Springer-Verlag: Berlin, 2008; Vol. 111, 720 pp.

(12) Lefebvre, J.; Austing, D. G.; Bond, J.; Finnie, P. Photoluminescence Imaging of Suspended Single-Walled Carbon Nanotubes. *Nano Lett.* **2006**, *6*, 1603–1608.

(13) Cherukuri, P.; Bachilo, S. M.; Litovsky, S. H.; Weisman, R. B. Near-Infrared Fluorescence Microscopy of Single-Walled Carbon Nanotubes in Phagocytic Cells. *J. Am. Chem. Soc.* **2004**, *126*, 15638–15639.

(14) Tsyboulski, D. A.; Bachilo, S. M.; Weisman, R. B. Versatile Visualization of Individual Single-Walled Carbon Nanotubes with Near-Infrared Fluorescence Microscopy. *Nano Lett.* **2005**, *5*, 975–979.

(15) Lefebvre, J.; Finnie, P. Polarized Photoluminescence Excitation Spectroscopy of Single-Walled Carbon Nanotubes. *Phys. Rev. Lett.* **2007**, *98*, 167406.

(16) Lefebvre, J.; Finnie, P. Excited Excitonic States in Single-Walled Carbon Nanotubes. *Nano Lett.* **2008**, *8*, 1890–1895.

(17) Cognet, L.; Tsyboulski, D. A.; Rocha, J.-D. R.; Doyle, C. D.; Tour, J. M.; Weisman, R. B. Stepwise Quenching of Exciton Fluorescence in Carbon Nanotubes by Single-Molecule Reactions. *Science* **2007**, *316*, 1465.

(18) Bachilo, S. M.; Strano, M. S.; Kittrell, C.; Hauge, R. H.; Smalley, R. E.; Weisman, R. B. Structure-Assigned Optical Spectra of Single-Walled Carbon Nanotubes. *Science* **2002**, *298*, 2361–2366.

(19) Lefebvre, J.; Fraser, J.; Homma, Y.; Finnie, P. Photoluminescence from single-walled carbon nanotubes: A comparison between suspended and micelle encapsulated nanotubes. *Appl. Phys. A: Mater. Sci. Proc.* **2004**, *78*, 1107–1110.

(20) Wang, F.; Sfeir, M. Y.; Huang, L.; Huang, X. M. H.; Wu, Y.; Kim, J.; Hone, J.; O'Brien, S.; Brus, L. E.; Heinz, T. F. Interactions between Individual Carbon Nanotubes Studied by Rayleigh Scattering Spectroscopy. *Phys. Rev. Lett.* **2004**, *96*, 167401.

(21) We estimate that τ_{ET} should be significantly shorter than τ_{PL}, the PL decay time with values between 10 and 200 ps. This would therefore imply that τ_{ET} would be less than 10 ps.

(22) Ma, Y.-Z.; Hertel, T.; Vardeny, Z. V.; Fleming, G. R.; Valkunas, L. In *Carbon Nanotubes: Advances Topics in the Synthesis, Structure, Properties and Applications, Topics in Applied Physics*; Jorio, A., Dresselhaus, G., Dresselhaus, M. S., Eds.; Springer-Verlag: Berlin, 2008; Vol. 111, pp 321−352.

(23) Oyama, Y.; Saito, R.; Sato, K.; Jiang, J.; Samsonidze, Ge. G.; Grüneis, A.; Miyauchi, Y.; Maruyama, S.; Jorio, A.; Dresselhaus, G.; Dresselhaus, M. S. Photoluminescence Intensity of Single-Wall Carbon Nanotubes. *Carbon* **2006**, *44*, 873–879.

(24) Tsyboulski, D. A.; Rocha, J.-D. R.; Bachilo, S. M.; Cognet, L.; Weisman, R. B. Structure-Dependent Fluorescence Efficiencies of Individual Single-Walled Carbon Nanotubes. *Nano Lett.* **2008**, *8*, 1270.

(25) Ohno, Y.; Kobayashi, A.; Kishimoto, S.; Maruyama, S.; Mizutani, T. Experimentally Evaluated (*n*,*m*) Dependence of Photoluminescence Efficiency of Single-Walled Carbon Nanotubes. Ninth International Conference on the Science and Application of Nanotubes Montpellier, France, 2008; p 111.

(26) Maarouf, A. A.; Kane, C. L.; Mele, E. J. Electronic Structure of Carbon Nanotube Ropes. *Phys. Rev. B* **2000**, *61*, 11156–11165.

JP810892Z